International Journal of Nanomedicine

Dovepress
open access to scientific and medical research

Open Access Full Text Article

ORIGINAL RESEARCH

RETRACTED ARTICLE: Alterations in the endometrium of rats, rabbits, and Macaca *mulatta* that received an implantation of copper/low-density polyethylene nanocomposite

This article was published in the following Dove Press journal:
International Journal of Nanomedicine
25 February 2014
Number of times this article has been viewed

Li-Xia Hu[1,*]
Hong Wang[1,*]
Meng Rao[1,*]
Xiao-Ling Zhao[1]
Jing Yang[1]
Shi-Fu Hu[1]
Jing He[1,2]
Wei Xia[1]
Hefang Liu[1]
Bo Zhen[1]
Haihong Di[1]
Changsheng Xie[3]
Xianping Xia[3]
Changhong Zhu[1]

[1]Family Planning Research Institute, Tongji Medical College, Huazhong University of Science and Technology, Wuhan, People's Republic of China; [2]Central Hospital of Wuhan, Wuhan, People's Republic of China; [3]Department of Materials Science and Engineering, Huazhong University of Science and Technology, Wuhan, People's Republic

*These authors contributed equally to this work

Correspondence: Changhong Zhu
Family Planning Research Institute, Tongji Medical College, Huazhong University of Science and Technology, 13 Hangkong Road, Wuhan 430030, People's Republic of China
Tel +86 27 8369 2651
Fax +86 27 8363 7374
Email reprodcentre@163.com

Abstract: A copper/low-density polyethylene nanocomposite (nano-Cu/LDPE), a potential intrauterine device component material, has been developed from our research. A logical extension of our previous work, this study was conducted to investigate the expression of plasminogen activator inhibitor-1 (PAI-1), substance P (SP), and substance P receptor (SP-R) in the endometrium of Sprague Dawley rats, New Zealand White rabbits, and *Macaca mulatta* implanted with nano-Cu/LDPE composite. The influence of the nano-Cu/LDPE composite on the morphology of the endometrium was also investigated. Animals were randomly divided into five groups: the sham-operated control group (SO group), bulk copper group (Cu group), LDPE group, and nano-Cu/LDPE groups I and II. An expression of PAI-1, SP, and SP-R in the endometrial tissues was examined by immunohistochemistry at day 30, 60, 90, and 180 post-implantation. The significant difference for PAI-1, SP, and SP-R between the nano-Cu/LDPE groups and the SO group ($P<0.05$) was identified when the observation period was terminated, and the changes of nano-Cu/LDPE on these parameters were less remarkable than those of the Cu group ($P<0.05$). The damage to the endometrial morphology caused by the nano-Cu/LDPE composite was much less than that caused by bulk copper. The nano-Cu/LDPE composite might be a potential substitute for conventional materials for intrauterine devices in the future because of its decreased adverse effects on the endometrial microenvironment.

Keywords: copper/low-density polyethylene nanocomposite, intrauterine device, side effects, endometrium

Introduction

As a safe and highly effective contraceptive, copper-bearing intrauterine devices (Cu-IUDs) have been increasingly used worldwide for population control.[1,2] It is well known that copper ions play an important role in the contraceptive mechanism of Cu-IUDs. On the one hand, the formation of cupric ions leads to spermicidal effects before fertilization and inhibitory effects of embryo implantation after fertilization.[3] On the other hand, copper enhances the possibility of local injury on the endometrium, including mechanical stimulation and sterile inflammation.[4] Large-scale epidemiologic studies indicate that adverse effects, such as spotting, pain, and intermenstrual bleeding, are still the main obstacles frequently associated with discontinuation of the Cu-IUDs.[5–7] All those adverse effects are most likely relevant to the burst release of copper ions in the first few months of usage. It has been demonstrated that a burst release of copper ions occurs in the first few months after insertion, and then the release rate

decreases and stabilizes gradually.[8] Therefore, controlling the release process of copper ions should be considered to maximize contraceptive efficacy and minimize adverse effects by preventing burst release rates at the initial period after insertion.

To lessen the adverse effects resulting from Cu-IUDs, a novel IUD material, copper/low-density polyethylene nanocomposite (nano-Cu/LDPE; patent number ZL200610124658.9) with various mass fractions of copper nanoparticles, has been prepared successfully. Briefly, the nano-Cu/LDPE composite is manufactured by physicochemical methods, combining high-quality copper nanoparticles, synthesized by heating and evaporation methods, and LDPE powders (Figure 1).[9] Copper nanoparticles are distributed in the composites uniformly, and the LDPE matrix is the frame. The spacing inside it offers osmosis passageway for copper ions and corrosion mediator, and it can effectively control the corrosion rate by separating the copper nanoparticles with the matrix; thus, it can control the copper ion release velocity. Its copper nanoparticles will convert into cupric ions when they meet with aqueous solutions such as water and simulated uterine solution.[10–12] When the cupric ions release and dissolve in uterine secretions, they can lead the spermatozoa to lose their activities and enhance the contraceptive efficacy of the Cu-IUD.[13]

Several observations in previous works were performed to explore whether this new composite can lessen adverse effects, as we hoped. In vitro tests for toxicity indicated that the nano-Cu/LDPE composite was very promising on histocompatibility.[14] The results of the experiment in rats demonstrated that the nano-Cu/LDPE composite had less effect on the endometrium prostaglandin E_2, tissue plasminogen activator (tPA), and angiogenesis-related factors levels than bulk copper.[15,16] A study on morphology also found that nano-Cu/LDPE composite had less influence on mouse endometrium ultrastructure than bulk copper.[17] The results indicate that this new material has low rates of adverse effects and reliable safety. However, the number of observations in previous work is very limited, and further research is needed.

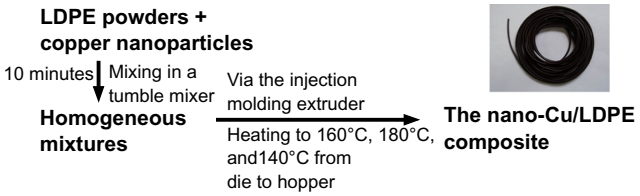

Figure 1 The flow chart of the nano-copper (Cu)/low-density polyethylene (LDPE) composite.

Following in the steps of a previous research series, we aimed to explore the alterations of nano-Cu/LDPE composite in the endometrial environment by evaluation of the relevant factors of fibrinolytic activity inhibitor, such as plasminogen activator inhibitor 1 (PAI-1), substance P (SP), and substance P receptor (SP-R) in different species (rat, rabbit, and *Macaca mulatta*). The influence of the nano-Cu/LDPE composite on the morphology of the endometrium was also investigated in the present work.

Materials and methods

IUD component materials

The IUD component materials were provided by the Department of Materials Science and Engineering of Huazhong University of Science and Technology, Wuhan, People's Republic of China. There were three different materials: bulk copper, LDPE, and nano-Cu/LDPE composite. The nano-Cu/LDPE composites were of two types: copper ions released at 5–10 μg and 11–20 μg/220 mm² per day. The nano-Cu/LDPE composite samples were prepared via our own patented techniques and has been introduced in our previous work.[9,18,19] The IUD component materials came in various sizes: surface areas of 4 mm² (used for Sprague Dawley [SD] rats), 20 mm² (for rabbits), and 35 mm² (for *M. mulatta*).

Animal treatment

Sexually mature female SD rats (weight range, 200–240 g) and New Zealand White rabbits (weight range, 2.5–3.0 kg) were obtained from the experimental animal center of Tongji Medical College, Huazhong University of Science and Technology. Sexually mature female *M. mulatta* weighing 4.8–8.1 kg, aged 4–12 years, were provided by the nonhuman primate experimental center (Fujian Family Planning Institute, Fuzhou, People's Republic of China). Animals were allowed to acclimatize for 1 week before carrying out the experiment and were bred under standard conditions. Drinking water and conventional feed were provided ad libitum. All protocols for animal care and treatment were approved by the Ethical Committee of Tongji Medical College, Huazhong University of Science and Technology.

One hundred and eight sexually mature female SD rats were recruited and randomly divided into five groups: the sham-operation group (SO group; n=12), the bulk copper group (Cu group; n=24), the LDPE group (n=24), and the nano-Cu/LDPE groups I (5–10 μg/220 mm² per day; n=24) and II (11–20 μg/220 mm² per day; n=24). Forty rabbits were randomly divided into five groups: the SO group, Cu group, LDPE group, and nano-Cu/LDPE groups I and II. Each group

had eight rabbits. Animals in the Cu, LDPE, and nano-Cu/LDPE groups were anesthetized, and the corresponding material was inserted into the caudal portion of unilateral uterine horn and secured to the uterine wall via operations including laparotomy and uterotomy. Likewise, 30 *M. mulatta* were divided into five groups. Each group had six animals. *M. mulatta* (3–5 days after menstruation) in the Cu, LDPE, and nano-Cu/LDPE groups were anesthetized, and then each corresponding material was inserted into the central portion of the uterus. Animals in the SO groups were treated with the same operations except for the insertion of the materials. During the experiment, animals were examined daily for any clinical signs and general abnormal appearances of the skin, awareness, motor activity, posture, muscle tone, reflexes, and autonomic features.

Determination of the PAI-1, SP, and SP-R levels in SD rats

The rats of each material-bearing group were divided into two subgroups (n=12), and the endometrial tissues were collected at days 90 and 180 after insertion. Because it was reported that the IUD in one uterine horn also changed the fibrinolytic activity of the contralateral horn,[5] instead of using the same animal's contralateral uterine horn as the control, 12 rats with SO treatment served as controls. Briefly, after anesthesia with 10% chloral hydrate (3 mg/kg intraperitoneally), the endometrial tissues of the material-bearing uterine horns (the uterine horns operated on in the SO group) were collected via laparotomy and uterotomy under aseptic conditions. Uterine tissue samples were cut into 5 mm pieces and gently washed with 0.8% physiological saline. Pieces were fixed immediately in 4% (w/v) paraformaldehyde (pH 7.2) for 14–16 hours at 4°C. Next, the samples were prepared for paraffin blocks by being dehydrated in gradient ethanol (70%, 75%, 80%, 95%, and 100%) and then immersed in cedar oil and paraffin. Serial 4–5 µm thick sections were prepared from the paraffin blocks and collected on glass slides that were processed for the streptavidin peroxidase (S-P) method of immunohistochemistry. Paraffin-embedded tissue sections were deparaffinized and rehydrated. Sections were treated with 3% H_2O_2 for 25 minutes to reduce nonspecific binding. Slides were washed in phosphate-buffered saline (PBS) and preincubated with normal nonimmune goat serum for 30 minutes at room temperature. The excess serum was blotted and the sections were incubated with rabbit-anti-rat anti-PAI-1 polyclonal antibody (Boster, Wuhan, People's Republic of China; 1:150 dilution), mouse-anti-rat anti-SP monoclonal antibody (Abcam, Cambridge, MA, USA; 1:1000 dilution), and rabbit-anti-rat anti-SP-R polyclonal antibody (LifeSpan Biosciences, Inc, Seattle, WA, USA; 1:200 dilution) for 1.5 hours at 37°C, respectively. After the slides were treated with the second biotinylated antibody, PBS, and S-P agents (Maixin, Fuzhou, People's Republic of China), the slides were visualized with 0.1% diaminobenzidine solution and then counterstained with hematoxylin. The slides were quickly dehydrated by ethanol, lucidificated by dimethylbenzene, and mounted with neutral gummi (Maixin). Slides were examined by light microscopy. The positive-stained cells were full of brown-yellow dye in the cytoplasm.

Determination of PAI-1, SP, and SP-R levels of New Zealand White rabbits

Rabbits were anesthetized with 3% pentobarbital sodium (1 mL/kg intravenously). Endometrial tissues of the material-bearing uterine (the uterine horns operated on in the SO group) were collected under aseptic conditions at day 60 after insertion. Primary antisera were goat-anti-rabbit anti-PAI-1 polyclonal antibody (Boster; 1:150 dilution), goat-anti-rabbit anti-SP polyclonal antibody (Boster; 1:150 dilution), and goat-anti-rabbit anti-SP-R polyclonal antibody (Boster; 1:150 dilution). Other experiential procedures and reagents except for the primary antibody were the same as SD rats.

Determination of PAI-1, SP, and SP-R levels of *M. mulatta*

M. mulatta were anesthetized with 10% chloral hydrate (10 mg/kg intravenously), and the endometrial tissues of the material-bearing uterine (the uterine center operated on in the SO group) were collected under aseptic conditions at day 30 after insertion. Primary antisera were rabbit-anti-human anti-PAI-1 polyclonal antibody (Boster; 1:150 dilution), mouse-anti-human anti-SP monoclonal antibody (Abcam; 1:1000 dilution), and rabbit-anti-human anti-SP-R polyclonal antibody (1:200 dilution). Other experimental procedures and reagents were the same as for SD rats.

Image analysis

Five visual fields for each slide were captured by the imaging system Olympus multifunction microscope (Olympus Corporation, Tokyo, Japan) with an application of cell measure procedures in the HMIAS-2003 high-definition color medical image analysis system (Qianping Image Co., Ltd, Wuhan, People's Republic of China); the expression of PAI-1, SP, and SP-R was analyzed with the average optical density value; and then the mean and standard deviation in each group were calculated.

Transmission and scanning electron microscopy analysis

Using these endometrial tissue samples, the morphologic features of endometrium were observed by transmission electron microscopy (TEM; Hitachi H-300; Hitachi Ltd, Tokyo, Japan) and scanning electron microscopy (SEM; JEOL, Tokyo, Japan).

Statistical analysis

SPSS 13.0 statistical software (SPSS Inc., Chicago, IL, USA) was used for statistical analysis. All values were expressed as mean ± standard deviation. The Student–Newman–Keuls test and Student's *t*-test were applied for statistical evaluation. A *P*-value of <0.05 was considered statistically significant.

Results

PAI-1, SP, and SP-R levels in rats

PAI-1 was expressed mainly on endochylema of vessel endothelial cells and epithelioglandular cells. Much obvious expression was observed in the endometrium of the SO group and nano-Cu/LDPE group I (Figure 2A and B). The PAI-1 of the Cu group was localized in part in the endochylema of vessel endothelial cells (Figure 2C). Likewise, SP (Figure 2D and E) and SP-R (Figure 2F and G) also, were expressed mainly on the endochylema of vessel endothelial cells and epithelioglandular cells; obvious expression was observed in the endometrium of the Cu group.

The optical density values of positive products within cells were measured and analyzed (Figure 3). At day 90 after insertion, there was no difference for PAI-1 expression among the nano-Cu/LDPE groups I and II and the Cu group ($P>0.05$), but expression was lower than that of the SO group ($P<0.05$). In comparison with the Cu group, the levels of SP in the nano-Cu/LDPE group and the LDPE and SO groups were significantly decreased ($P<0.05$). The SP-R expression of the nano-Cu/LDPE groups and the LDPE group was higher than that of the SO group ($P<0.05$) but lower than that of the Cu group ($P<0.05$). At day 180 after insertion, no difference of PAI-1 expression in all

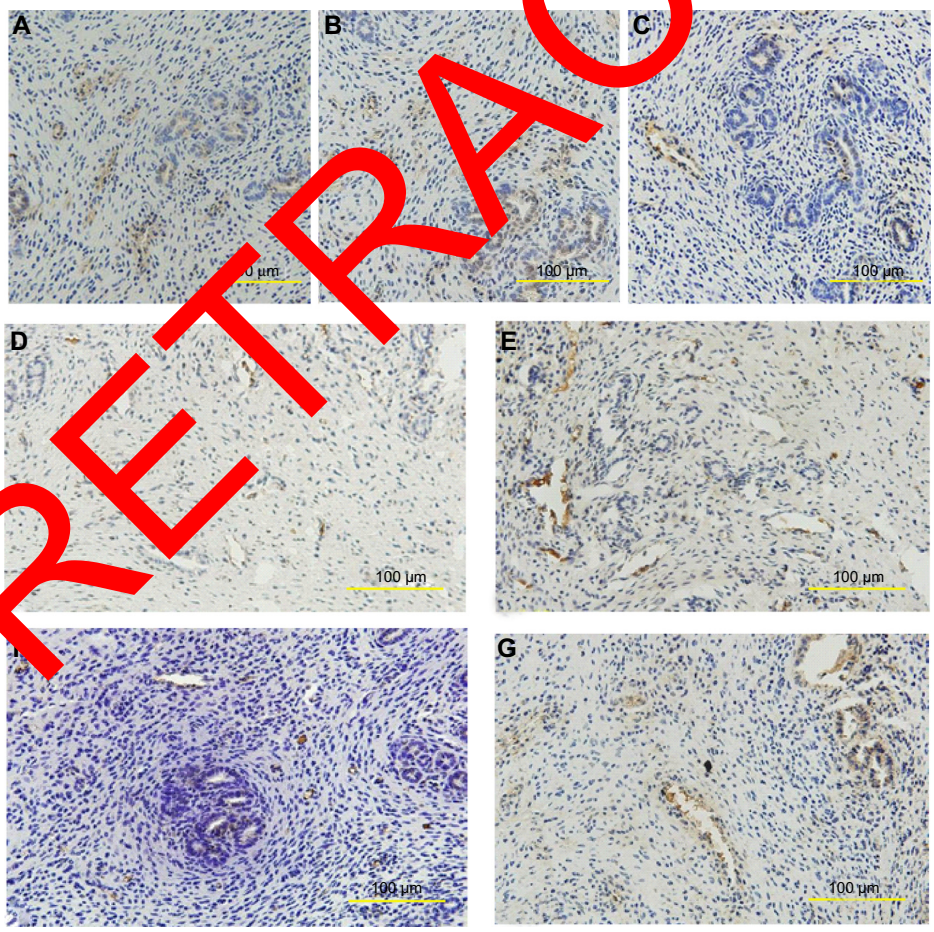

Figure 2 Distribution of plasminogen activator inhibitor I (PAI-1), substance P (SP), and substance P receptor (SP-R) in the endometrium of rats. At the 90th day after insertion, the tissues obtained from endometrium were examined by immunohistochemistry. (**A**) PAI-1 of the sham-operated control group. (**B**) PAI-1 of the nano-copper (Cu)/low-density polyethylene (LDPE) group I. (**C**) PAI-1 of the Cu group. (**D**) SP of the nano-Cu/LDPE group I. (**E**) SP of the Cu group. (**F**) SP-R of the nano-Cu/LDPE group I. (**G**) SP-R of the Cu group.

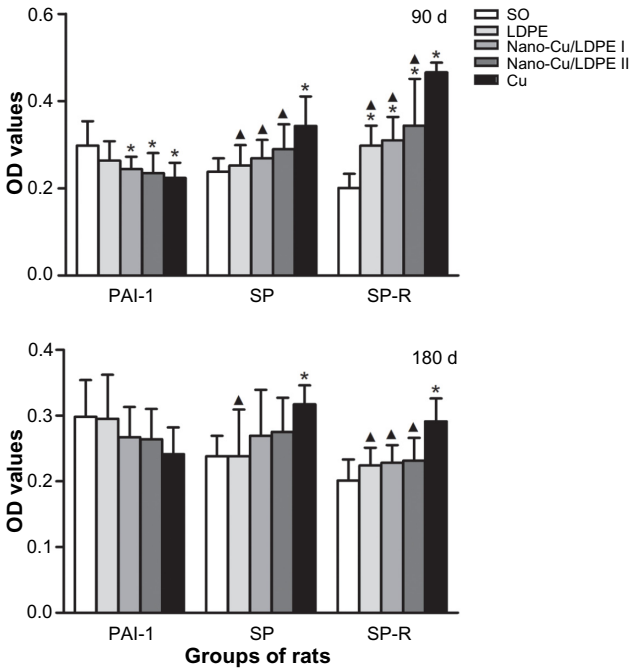

Figure 3 Plasminogen activator inhibitor 1 (PAI-1), substance P (SP), and substance P receptor (SP-R) levels in rats at day 90 and day 180 after insertion (optical density [OD], mean ± standard deviation).
Notes: Compared with the sham-operated control group, *$P<0.05$. Compared with the copper (Cu) group, ▲$P<0.05$.
Abbreviations: SO, sham-operated control group; LDPE, low-density polyethylene; d, days.

material-bearing groups was observed ($P>0.05$). Compared with that of the SO group, the SP level of the Cu group was significantly increased ($P<0.05$). There was no difference in SP-R levels among all groups except for the Cu group. From 90 to 180 days after insertion, PAI-1 and SP contents were not significantly different in the same group ($P>0.05$), but an obvious decrease in SP-R expression for each experimental group was observed ($P<0.05$).

PAI-1, SP, and SP-R levels in rabbits

PAI-1 was mainly expressed around the endometrial blood vessels, in the cytoplasm of smooth muscle cells, and in some epithelioglandular cells (Figure 4A–C). SP (Figure 4D) and SP-R (Figure 4F) of the nano-Cu/LDPE group I were revealed in a few vessel endothelial cells and smooth muscle cells. SP (Figure 4E) and SP-R (Figure 4G) of the Cu group were mainly observed around endometrial blood vessels, and some in the cytoplasm of smooth muscle cells.

Figure 5 shows the PAI-1, SP, and SP-R levels of rabbits. At day 60 after insertion, there was no difference for PAI-1 expression between the SO group, LDPE group, and nano-Cu/LDPE group I ($P>0.05$). The level in the nano-Cu/LDPE group II was significantly lower than that in the SO group ($P<0.05$) but was higher than in the Cu group ($P<0.05$). The SP levels of the nano-Cu/LDPE groups were higher than that of the SO group ($P<0.05$) but were obviously lower than that of the Cu group ($P<0.05$). The expression levels of SP-R in the nano-Cu/LDPE groups were significantly higher than in the SO and LDPE groups ($P<0.05$) and were obviously lower than in the Cu group ($P<0.05$). However, the SP-R level in the nano-Cu/LDPE group II was significantly higher than in group I ($P<0.05$).

PAI-1, SP, and SP-R levels in *M. mulatta*

PAI-1 was mainly expressed around the endometrial blood vessels, in the cytoplasm of smooth muscle cells, and in some epithelioglandular cells (Figure 6A–C). SP (Figure 6D and E) and SP-R (Figure 6F and G) were mainly observed around endometrial blood vessels, sometimes in the cytoplasm of smooth muscle cells.

Figure 7 shows the PAI-1, SP, and SP-R levels of *M. mulatta* at day 30 after insertion, the levels of PAI-1 in nano-Cu/LDPE groups were significantly lower than that in the SO group ($P<0.05$) but higher than in the Cu group ($P<0.05$). In addition, the PAI-1 level in nano-Cu/LDPE group I was significantly higher than in group II ($P<0.05$). Compared with the SO group, the concentrations of SP in all material-bearing groups except for the LDPE group were significantly increased ($P<0.05$), and these parameters in the nano-Cu/LDPE groups were significantly lower than in the Cu group ($P<0.05$), but the SP level of nano-Cu/LDPE group II was significantly higher than group I ($P<0.05$). The SP-R expression of nano-Cu/LDPE groups was higher than that in the SO group and LDPE group ($P<0.05$) but lower than in the Cu group ($P<0.05$).

Morphology of endometrium

The TEM images of the endometrial ultrastructure for the rats that received implants for 90 days are presented in Figure 8. The ultrastructure of endometrium of the SO group rats (Figure 8A) can be seen such that no obvious abnormity was found in the morphology and structure of epithelia and that the junction of cells can be observed normally. In the LDPE group (Figure 8B), the structure of endometrial cells was close to normal, and the gap of some of the stromal cells became larger. The ultrastructure of the endometrium in the nano-Cu/LDPE group I is shown in Figure 8C and D. In the mass, the structure of endometrial cells was close to normal. In Figure 8C, one can see that the microvilli of endometrial epithelial cells became shorter and sparser. In Figure 8D, the lysosome in the epithelial cells increased slightly. The ultrastructure of endometrium of the nano-Cu/LDPE group II is shown in Figures 8E and F. The endoplasmic reticulum

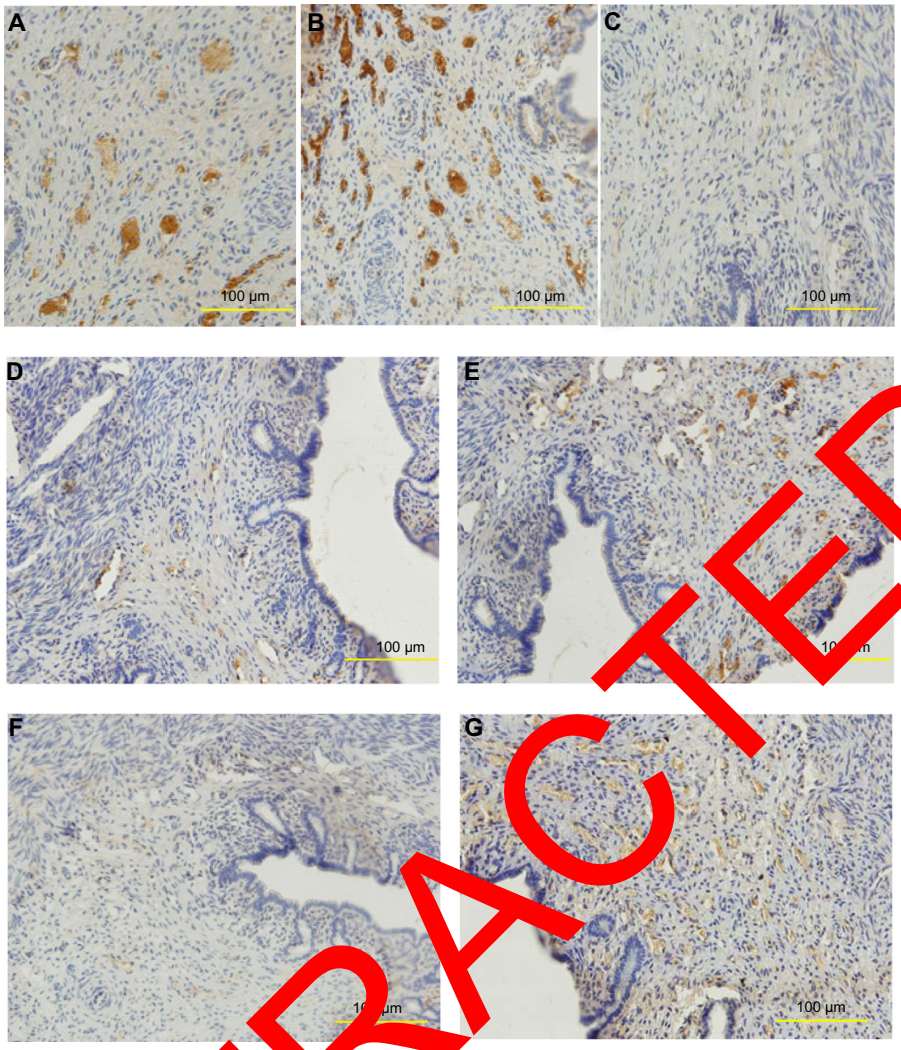

Figure 4 Distribution of plasminogen activator inhibitor I (PAI-I), substance P (SP), and substance P receptor (SP-R) in the endometrium of rabbits. (**A**) PAI-I of the sham-operated control group. (**B**) PAI-I of the nano-Cu (Cu)/low-density polyethylene (LDPE) group I. (**C**) PAI-I of the Cu group. (**D**) SP of the nano-Cu/LDPE group I. (**E**) SP of the Cu group. (**F**) SP-R of the nano-Cu/LDPE group I. (**G**) SP-R of the Cu group.

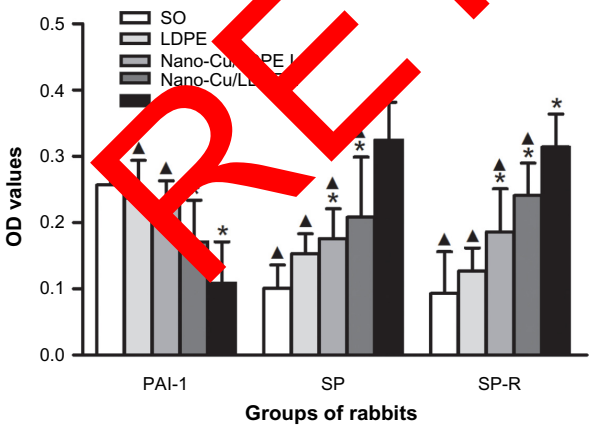

Figure 5 Plasminogen activator inhibitor I (PAI-I), substance P (SP), and substance P receptor (SP-R) levels in rabbits at day 60 after insertion (optical density [OD], mean ± standard deviation).
Notes: Compared with the sham-operated control (SO) group. *$P<0.05$. Compared with the copper (Cu) group, ▲$P<0.05$.
Abbreviation: LDPE, low-density polyethylene.

in the epithelial cells expanded slightly. In Figure 8E, one can see that the microvilli became shorter, larger, and sparser. In Figure 8F, the lysosome in the epithelial cells increased significantly. The ultrastructure of endometrium of the Cu group is shown in Figure 8G and H. In Figure 8G, it can be seen that the endoplasmic reticulum of the epithelial cells expanded obviously; it also can be seen that the junction of cells disappeared, the outline of the cells was obscured, the microvilli of the epithelial cells became shorter and larger, and some of the microvilli were broken off. In Figure 8H, it can be seen that the mitochondria have already been deformed seriously and that some of the cells in the stroma collapsed.

The SEM and TEM images of endometrial ultrastructure for the rabbits are presented in Figure 9. In the SEM images, the endometrial mucosal surface of the SO group (Figure 9A) was lined by secretory cells and isolated groups of ciliated

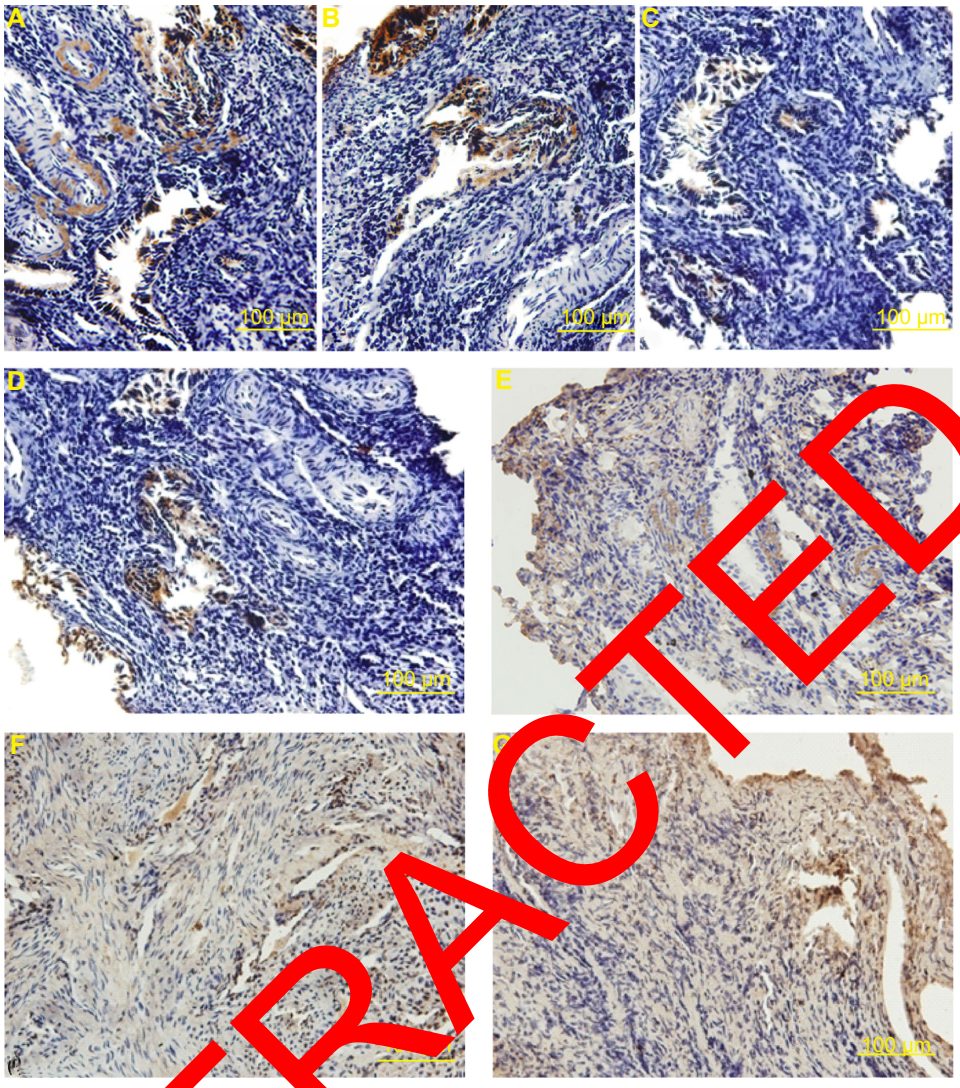

Figure 6 Distribution of plasminogen activator inhibitor I (PAI-I), substance P (SP), and substance P receptor (SP-R) in the endometrium of *Macaca mulatta*. (**A**) PAI-I of the sham-operated control group. (**B**) PAI-I of the nano-copper (Cu)/low-density polyethylene (LDPE) group I. (**C**) PAI-I of the Cu group. (**D**) SP of the nano-Cu/LDPE group I. (**E**) SP of the Cu group. (**F**) SP-R of the nano-Cu/LDPE group I. (**G**) SP-R of the Cu group.

cells and exhibits many glandular openings. Secretory cells were characterized by a moderate number of microvilli. Changes in the morphology of the endometrium were slight in the LDPE and nano-Cu/LDPE I groups (Figure 9B and C). In Figure 9D (the nano-Cu/LDPE group II), secretory cells lining the uterine mucosa became larger and were characterized by a sparse population of short microvilli. In Figure 9E (Cu group), it can be seen that the surface morphology of endometrial mucosal surface changed dramatically. The secretory cells, which have lost microvilli, exhibited a rather smooth surface and were in the process of sloughing off. The luminal openings of endometrial glands were irregular, and ciliated cells were apparently decreased. In the TEM images, the ultrastructure of endometrium of the SO group of rabbits is shown in Figure 9A. It can be seen that no obvious abnormity was found in the morphology and structure of endometrial epithelia and that the junction of cells can be observed normally. In the LDPE group (Figure 9B), the structure of endometrial cells was close to normal and the microvilli of epithelial cells became sparser. In Figure 9C (the nano-Cu/LDPE group I), the microvilli of epithelial cells became shorter and sparser and the endoplasmic reticulum in epithelial cells expanded slightly. In Figure 9D (the nano-Cu/LDPE group II), the endoplasmic reticulum of the epithelial cells expanded obviously and the mitochondria swelled. It also can be seen that the junction of cells appeared. In the Cu group (Figure 9E), the microvilli of epithelial cells became shorter and larger, and some of the microvilli were broken off. The endoplasmic reticulum of epithelial cells expanded obviously, and the mitochondria deformed seriously. It also

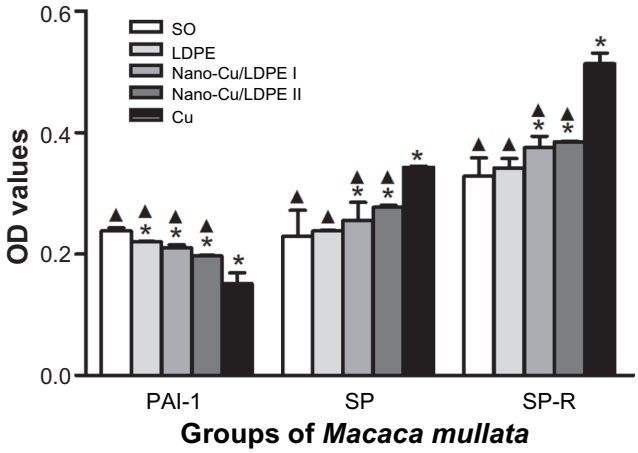

Figure 7 Plasminogen activator inhibitor I (PAI-I), substance P (SP), and substance P receptor (SP-R) levels in *Macaca mulatta* at day 30 after insertion (optical density [OD], mean ± standard deviation).
Notes: Compared with the sham-operated control (SO) group, *$P<0.05$. Compared with the copper (Cu) group, ▲$P<0.05$.
Abbreviation: LDPE, low-density polyethylene group.

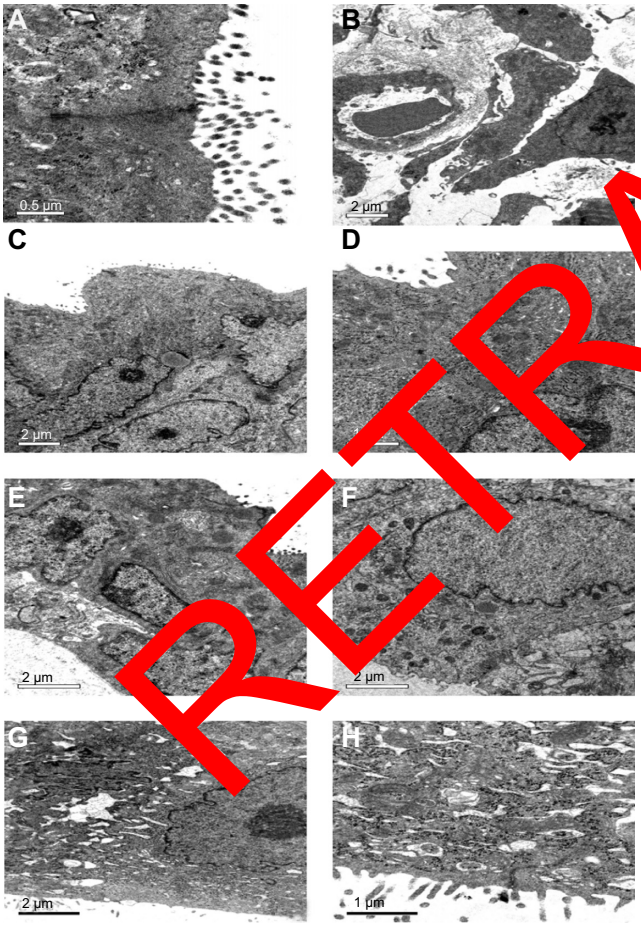

Figure 8 Transmission electron microscope images of endometrial ultrastructure for the rats. (**A**) The sham-operated control group. (**B**) the low-density polyethylene (LDPE) group. (**C** and **D**) the nano-copper (Cu)/LDPE group I. (**E** and **F**) the nano-Cu/LDPE group II. (**G** and **H**) the Cu group. It can be seen that the damage to the endometrium of rat caused by the bulk copper is more serious than that caused by the nano-Cu/LDPE composite.

can be seen that the junction of the cells was deformed and the outline of the cells was obscured.

The TEM images of the endometrial ultrastructure for the *M. mulatta* that received implants for 30 days are presented in Figure 10. The ultrastructure of endometrium of the SO group of *M. mulatta* is shown in Figure 10A. It can be seen that no obvious abnormity was found in the epithelia and that the junction of cells can be observed normally. In the LDPE group (Figure 10B), the structure of endometrial cells was close to normal, and vacuoles appeared in the cytoplasm. The ultrastructure of the endometrium of the nano-Cu/LDPE group I is shown in Figure 10C. The microvilli of endometrial epithelial cells became shorter and sparser. In Figure 10D (the nano-Cu/LDPE group II), one can see that the gap of some of the endometrial epithelial cells became wider. The ultrastructure of the endometrium of the Cu group is shown in Figure 10E and F. In Figure 10E, the feature structures of the endometrial cells have already been disordered, and some of the cells show necrosis and shedding. It also can be seen that the gap between cells widened significantly. In Figure 10F, it can be seen that the mitochondria have already been deformed seriously.

Discussion

Rodents, such as rats, mice, and rabbits, have frequently been employed for studies on the influence of different IUDs on the endometrium.[20,21] The uterus of these animals consists of two long uterine horns and a short common part. The presence of a paired genital tract offers special experimental possibilities. The genetic and physiological similarities between the rhesus macaque (*M. mulatta*) and humans make the former an excellent model for clinically relevant biomedical research.[22,23]

The balance between tPA and PAI-1 plays an important role in the maintenance of normal hemokinesis. An increase in tPA or decrease in PAI-1 results in the accentuation of fibrinolytic activity and hemorrhage. A prior study from this laboratory demonstrated that tPA levels in nano-Cu/LDPE groups were slightly increased and that the effects of the nano-Cu/LDPE composite on tPA levels in the endometrium were slighter than those of traditional bulk copper. PAI-1 is a member of the serpin (serine protease inhibitor) superfamily of proteins[24] and is expressed by many different cell types in a variety of tissues.[25] After secretion in its active conformation, PAI-1 can form stable covalent complexes with tPA and thereby irreversibly block the activity of tPA.[26,27] PAI-1 messengerRNA and protein are localized in endometrial epithelium and stromal cells around small blood vessels.[28] SP is thought to play important roles in the

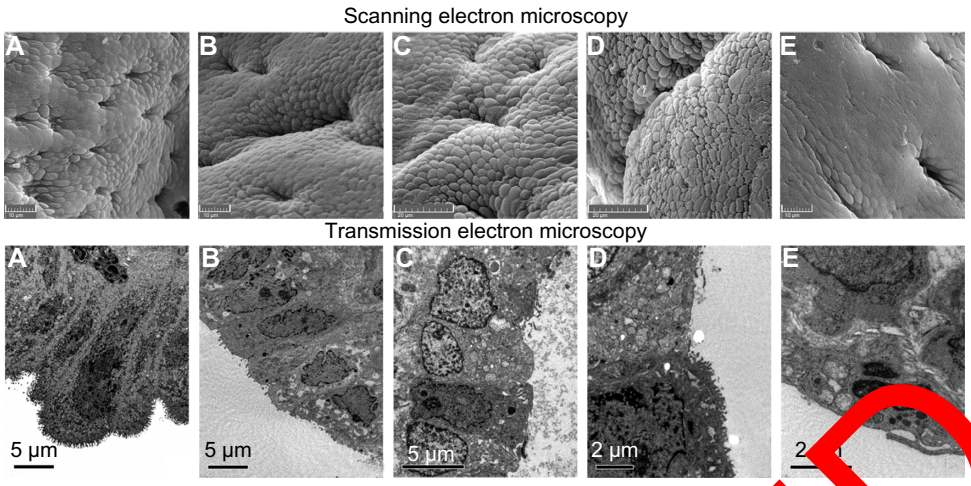

Figure 9 Scanning electron microscope images of endometrial ultrastructure for the rabbits. (**A**) The sham-operated control (SO) group, (**B**) the low-density polyethylene (LDPE) group, (**C**) the nano-copper (Cu)/LDPE group I, (**D**) the nano-Cu/LDPE group II, (**E**) the Cu group. Transmission electron microscope images: (**A**) the SO group, (**B**) the LDPE group, (**C**) the nano-Cu/LDPE group I, (**D**) the nano-Cu/LDPE group II, and (**E**) the Cu group.

control of myometrial contractility[29] and uterine blood flow.[30] SP-R, a G-protein-coupled receptor, plays a critical role in injury-induced hyperalgesia or pain.[31,32] SP interacts with the SP-R to produce its postsynaptic effects.[33] SP and SP-R have been located in the adventitia of large uterine vessels in the myometrium and small vessels of the myometrium and endometrium in different species.[34]

The results of this study are similar to those of relevant research. PAI-1, SP, and SP-R are mainly expressed around the endometrial blood vessels and in the cytoplasm of smooth muscle cells and some epithelioglandular cells in rats, rabbits, and *M. mulatta*. From 30 to 180 days after insertion, the effects of the nano-Cu/LDPE composite on PAI-1, SP, and SP-R levels in the endometrium were less remarkable than those of conventional bulk copper. At day 180 after insertion, no differences of PAI-1, SP and SP-R expression in all material-bearing groups except the Cu group were observed. On the one hand, the results support the evidence that the effects of the endometrial microenvironment take place within the first few months after material insertion. On the other hand, the effects of the nano-Cu/LDPE composite on PAI-1, SP, and SP-R levels in the endometrium are slighter than those of the bulk copper. From the morphologic features of the endometrium of the rats, rabbits, and *M. mulatta*, a conclusion can be drawn that the damage of the endometrium of the animals caused by the nano-Cu/LDPE composite is much less than that caused by bulk copper.

The contraceptive effect of the Cu-IUD is mainly dependent on the copper ions released by the corrosion of copper;[35–39] the larger the release rate of cupric ions, the better the contraceptive effect. According to the literature, there is an extremely high corrosive rate during the first few months, known as a cupric ion "burst release" after Cu-IUD insertion.[8] However, overexposure could produce a wide spectrum of effects on surrounding cells and may exert significant in situ adverse effects. Adverse effects such as heavy bleeding and

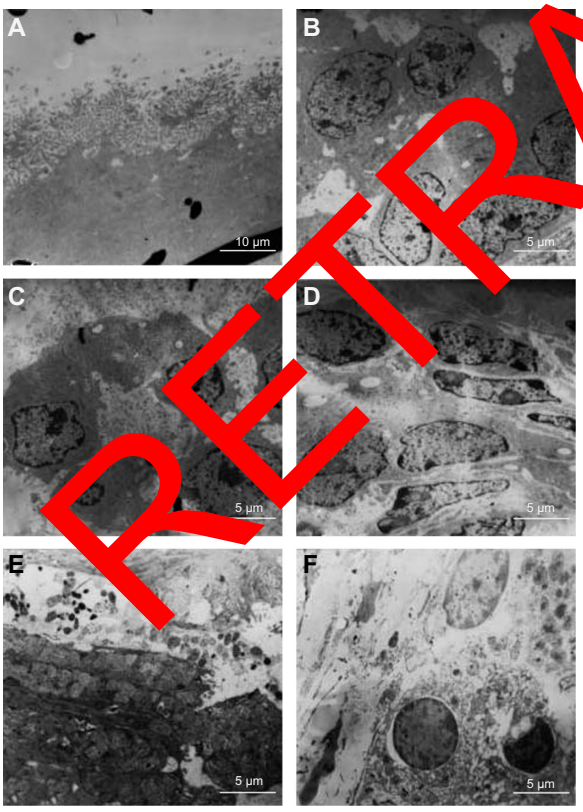

Figure 10 Transmission electron microscope images of endometrial ultrastructure for the *Macaca mulatta*. (**A**) The sham-operated control (SO) group, (**B**) the low-density polyethylene (LDPE) group, (**C**) the nano-copper (Cu)/LDPE group I, (**D**) the nano-Cu/LDPE group II, (**E** and **F**) the Cu group.

pelvic pain reported after IUD implant may be related to the inflammation processes associated with high copper ion levels. It is suggested that the cellular and biochemical changes occur in the endometrium after Cu-IUD insertion.[40–42] Findings from several in vitro and in vivo assays provide evidence that copper ions are capable of interacting directly with macromolecules, modifying conformational structures and thus causing site-specific damage,[43–45] and indirectly catalyzing through the Fenton/Haber-Weiss reaction the formation of reactive oxygen species and causing several cellular alterations.[46–48] In addition, ions from metals such as copper exhibit a high affinity for thiol groups and may therefore severely disturb many cell metabolic functions.[49] As a consequence, oxidative stress, which is the state of redox disequilibrium in which reactive oxygen species production overwhelms the antioxidant defense capacity of the cell, may lead to adverse biological consequences such as damage to lipids, DNA, or proteins, resulting in excess cell proliferation, apoptosis, or mutagenesis.[50]

Recently, the work of Araya et al shows that the sperm motility almost decreased to zero at a cupric ion concentration of ~8×10^{-6} mol/L (~0.5 µg/mL) for a period of ~20 minutes.[13] Indicating that 1.0 µg/mL of the cupric ion concentration is enough to inhibit the motility of human sperm in a simulated uterine solution even if half of the released cupric ions were absorbed by endometrium in vivo. Therefore, 1.0 µg/mL can be considered the minimal cupric ion concentration that needs to ensure contraceptive efficacy of the IUD in clinical use. The entire genital tract is reported to be exposed to 25–80 µg/day of cupric ions released from a inserted Cu-IUD.[6,8,51] That is to say, the cupric ion concentration released by the existing Cu-IUD in uterine fluid is apparently much larger than the minimal cupric ion concentration needed to ensure contraceptive efficacy.

To decrease the adverse effects of the existing Cu-IUD, a brand-new IUD material, we have successfully prepared the nano-Cu/LDPE composite. Not only the special effects of cupric ions, but also the controlled release technology contributes to nano-Cu/LDPE composite preparation. Compared with conventional Cu-IUDs, the nano-Cu/LDPE composite has unique characteristics. The LDPE matrix is the frame, and copper nanoparticles are distributed in the composites uniformly. The space inside offers osmosis passageway for copper ions and corrosion mediator, and it can effectively control the corrosion rate by separating the copper nanoparticles with the matrix. The prophase of study confirms that the material releases copper ions in a steady velocity in a simulated uterine solution, which differs from the burst release of copper ions of conventional Cu-IUDs.[18,40,41,52] The size effect of copper nanoparticles can control copper ion release velocity.[53] With the same copper content, the nano-Cu/LDPE IUD releases more copper ions than the conventional Cu-IUD in the same liquid environment. The antifertility effect of the nano-Cu/LDPE composite is as excellent as that of the Cu-IUD material.[15] Furthermore, comparison of results obtained from cytotoxic effect in vitro shows that cytotoxicity caused by the Cu-IUD is significantly higher than that caused by the nano-Cu/LDPE IUD.[14] Therefore, in this work, because of the unique characteristics of the nano-Cu/LDPE composite, the cupric ion concentration is apparently smaller than that of the bulk copper, possibly explaining why the effects of the nano-Cu/LDPE composite on PAI-1, SP, and SP-R levels in the endometrium are less remarkable than those of bulk copper.

Among the various factors that can cause damage to the endometrium of animals, the surface condition of the Cu-IUD material may be an important factor except for the influence of the release rate of cupric ions.[40] The surface of the bulk copper of the existing Cu-IUDs becomes coarser and coarser with increasing time in the uterine solution, because of the corrosion of copper.[54] Finally, the corrosion products, such as Cu_2O, $Cu(OH)_2$, and $CaCO_3$, are deposited on the surface of the bulk copper; such hard, calcified deposits as $CaCO_3$ will aggravate the damage of the endometrium.[55,56] Compared with corroded bulk copper, the surface of the corroded nano-Cu/LDPE composite is much smoother, much softer, and much cleaner.[17] Therefore, the damage caused by the implanted nano-Cu/LDPE composite is much less than that caused by implanted bulk copper.

Conclusion

In view of these study results, the effects of the nano-Cu/LDPE composite on the corresponding factors involved in irregular bleeding and pain after insertion are slighter than those of bulk copper, and its mechanism of reducing the adverse effects of an IUD might be related to a slight decrease in PAI-1 and to the inhibition of local SP and SP-R level increases after insertion. More importantly, the nano-Cu/LDPE composite and bulk copper have different influences on the morphology of endometrium of animals. The damage of the endometrium caused by nano-Cu/LDPE composite is much less than that caused by the bulk copper. These data are in accordance with our previous work showing that this new type of composite, the nano-Cu/LDPE composite, may be a potential substitute for conventional materials for IUDs in the future because of its decreased adverse effects on the endometrial microenvironment. In addition, further investigation has to be done in adequate clinical trials to test the effect of

this novel material on human endometrium and to determine whether there is any reduction in adverse effects.

Acknowledgment

The authors gratefully acknowledge the financial support of Key Technologies Research and Development Programme of the National Tenth Five Years Plan, People's Republic of China (number 2006BA103B01).

Disclosure

The authors report no conflicts of interest in this work.

References

1. Trussell J. Understanding contraceptive failure. *Best Pract Res Clin Obstet Gynaecol*. 2009;23(2):199–209.
2. Mansour D, Inki P, Gemzell-Danielsson K. Efficacy of contraceptive methods: A review of the literature. *Eur J Contracept Reprod Health Care*. 2010;15(1):4–16.
3. Spinnato JA 2nd. Mechanism of action of intrauterine contraceptive devices and its relation to informed consent. *Am J Obstet Gynecol*. 1997;176(3):503–506.
4. Johannisson E. Mechanism of action of intrauterine devices: biochemical changes. *Contraception*. 1987;36(1):11–22.
5. Lee NC, Rubin GL, Ory HW, Burkman RT. Type of intrauterine device and the risk of pelvic inflammatory disease. *Obstet Gynecol*. 1983;62(1):1–6.
6. Timonen H. Copper release from Copper-T intrauterine devices. *Contraception*. 1976;14(1):25–38.
7. Mora N, Cano E, Mora EM, Bastidas JM. Influence of pH and oxygen on copper corrosion in simulated uterine fluid. *Biomaterials*. 2002;23(3):667–671.
8. Arancibia V, Peña C, Allen HE, Lagos G. Characterization of copper in uterine fluids of patients who use the copper T-380A intrauterine device. *Clin Chim Acta*. 2003;332(1–2):69–
9. Cai S, Xia X, Xie C. Corrosion behavior of copper/LDPE nanocomposites in simulated uterine solution. *Biomaterials*. 2005;[illegible]15):2671–2676.
10. Cai S, Xia X, Xie CS. Research on [illegible]+ transformation of Cu and its oxides particles with different sizes in simulated uterine solution. *Corrosion Sci*. 2005;47(4):1039–1047.
11. Xia X, Xie C, Cai S, Yan[illegible], Yang X. Corrosion characteristics of copper microparticles and copper nanoparticles in distilled water. *Corrosion Sci*. 2006;48(12):[illegible]4–3932.
12. Xia X, Tang Y, Xie C, Wang Y, Cai S, Zhu C. An approach to give prospective [illegible]pan on the copper/low-density-polyethylene nanocomposite intrauterine device. *J Mater Sci Mater Med*. 2011;22(7):1773–1781.
13. Araya[illegible] Gómez[illegible] Vera R, Bastidas JM. Human spermatozoa motility and lysis in a Ringer's solution containing cupric ions. *Contraception*. 2003;67(2):161–163.
14. Hu LX, He J, [illegible]u L, et al. Biological evaluation of the copper/low-density polyethylene nanocomposite intrauterine device. *PLoS One*. 2013;8(9):e74128.
15. Liu HF, Liu ZL, Xie CS, Yu J, Zhu CH. The antifertility effectiveness of copper/low-density polyethylene nanocomposite and its influence on the endometrial environment in rats. *Contraception*. 2007;75(2):157–161.
16. Li J, Liu Z, Li S, et al. Correlative investigation of copper/low-density polyethylene nanocomposite on the endometrial angiogenesis in rats. *Front Med China*. 2007;1(4):401–404.
17. Xia X, Xie C, Zhu C, Cai S, Yang X. Effect of implanted Cu/low-density polyethylene nanocomposite on the morphology of endometrium in the mouse. *Fertil Steril*. 2007;88(2):472–478.
18. Xu T, Lei H, Cai SZ, Xia XP, Xie CS. The release of cupric ion in simulated uterine: New material nano-Cu/low-density polyethylene used for intrauterine devices. *Contraception*. 2004;70(2):153–157.
19. Xia XP, Cai SZ, Xie CS. Preparation, structure and thermal stability of Cu/LDPE nanocomposites. *Mater Chem Phys*. 2006;95:122–129.
20. Liedholm P, Sjöberg NO. Differences in effect of copper and ProgestasertR IUDS on fibrinolytic activity of the endometrium in the rabbit. *Contraception*. 1979;19(5):443–448.
21. Al-Amood WS, Al-Khateeb E, Chatterjee R, Chatterjee A. Intrauterine contraceptive devices: failure of unilateral intrauterine device in inducing luteolysis in rabbits, rats and mice. *Contraception*. 1981;23(5):543–548.
22. Pennisi E. Boom time for monkey research. *Science*. 2007;316(5822):216–218.
23. Pennisi E. Genomicists tackle the primate[illegible] *Science*. 2007;316(5822):218–221.
24. Pannekoek H, Veerman H, Lambe[illegible]s H, et al. Endothelial plasminogen activator inhibitor (PAI): a new member of the Serpin gene family. *EMBO J*. 1986;5(10):2539–2544.
25. Simpson AJ, Booth NA, Moore NR, Bennett B. Distribution of plasminogen activator inhibitor (PAI-1) in tissues. *Hum Pathol*. 1991;44(2):139–143.
26. Gils A, Declerck PJ. Structure-function relationships in serpins: current concepts and controversies. *Thromb Haemost*. 1998;80(4):531–541.
27. Van De[illegible]B, Scroyen I, W[illegible]C, et al. Maximal PAI-1 inhibition in vivo requires neutralizing antibodies that recognize and inhibit glycosylated PAI-1. *Thromb Res*. 2012;129(4):e126–e133.
28. [illegible]ngren J, Pilka [illegible]Noskova V, et al. Differential localization and expression of urokinase plasminogen activator (uPA), its receptor (uPAR), and its inhibitor (PAI-1) mRNA and protein in endometrial tissue during the menstrual cycle. *Mol Hum Reprod*. 2004;10(9):655–663.
29. Mukai H, [illegible]naka H, Goto K, Kawai K, Yamashita K, Munekata E. Structure-activity relationships of mammalian bombesin-like neuropeptides in the contraction of rat uterus. *Neuropeptides*. 1991;19(4):[illegible]3–250.
30. Ekesbo R, Alm P, Ekström P, Lundberg LM, Akerlund M. Innervation of the human uterine artery and contractile responses to neuropeptides. *Gynecol Obstet Invest*. 1991;31(1):30–36.
31. Khasabov SG, Rogers SD, Ghilardi JR, Peters CM, Mantyh PW, Simone DA. Spinal neurons that possess the substance P receptor are required for the development of central sensitization. *J Neurosci*. 2002;22(20):9086–9098.
32. Vera-Portocarrero LP, Zhang ET, King T, et al. Spinal NK-1 receptor expressing neurons mediate opioid-induced hyperalgesia and antinociceptive tolerance via activation of descending pathways. *Pain*. 2007;129(1–2):35–45.
33. Bae SE, Corcoran BM, Watson ED. Immunohistochemical study of the distribution of adrenergic and peptidergic innervation in the equine uterus and the cervix. *Reproduction*. 2001;122(2):275–282.
34. Pennefather JN, Patak E, Pinto FM, Candenas ML. Mammalian tachykinins and uterine smooth muscle: the challenge escalates. *Eur J Pharmacol*. 2004;500(1–3):15–26.
35. Bastidas JM, Cano E, Mora N. Copper corrosion-simulated uterine solutions. *Contraception*. 2000;61(6):395–399.
36. Mishell DR Jr. Intrauterine devices: mechanisms of action, safety, and efficacy. *Contraception*. 1998;58(Suppl 3):45S–53S; quiz 70S.
37. Thiery M. Intrauterine contraception: from silver ring to intrauterine contraceptive implant. *Eur J Obstet Gynecol Reprod Biol*. 2000;90(2):145–152.
38. Westhoff CL. Current assessment of the use of intrauterine devices. *J Nurse Midwifery*. 1996;41(3):218–223.
39. Zipper JA, Tatum HJ, Pastene L, Medel M, Rivera M. Metallic copper as an intrauterine contraceptice adjunct to the "T" device. *Am J Obstet Gynecol*. 1969;105(8):1274–1278.
40. Patai K, Szilagyi G, Noszal B, Szentmariay I. Local tissue effects of copper-containing intrauterine devices. *Fertil Steril*. 2003;80(5):1281–1283.

41. Grillo CA, Reigosa MA, de Mele MA. Does over-exposure to copper ions released from metallic copper induce cytotoxic and genotoxic effects on mammalian cells? *Contraception*. 2010;81(4):343–349.
42. Stanback J, Grimes D. Can intrauterine device removals for bleeding or pain be predicted at a one-month follow-up visit? A multivariate analysis. *Contraception*. 1998;58(6):357–360.
43. Burkitt MJ. Copper – DNA adducts. *Methods Enzymol*. 1994;234: 66–79.
44. Kang J, Lin C, Chen J, Liu Q. Copper induces histone hypoacetylation through directly inhibiting histone acetyltransferase activity. *Chem Biol Interact*. 2004;148(3):115–123.
45. Letelier ME, Lepe AM, Faúndez M, et al. Possible mechanisms underlying copper-induced damage in biological membranes leading to cellular toxicity. *Chem Biol Interact*. 2005;151(2):71–82.
46. Pourahmad J, O'Brien PJ. A comparison of hepatocyte cytotoxic mechanisms for Cu2+ and Cd2+. *Toxicology*. 7, 2000;143(3): 263–273.
47. Gaetke LM, Chow CK. Copper toxicity, oxidative stress, and antioxidant nutrients. *Toxicology*. 2003;189(1–2):147–163.
48. Moriwaki H, Osborne MR, Phillips DH. Effects of mixing metal ions on oxidative DNA damage mediated by a Fenton-type reduction. *Toxicol In Vitro*. 2008;22(1):36–44.
49. Hultberg B, Andersson A, Isaksson A. Copper ions differ from other thiol reactive metal ions in their effects on the concentration and redox status of thiols in HeLa cell cultures. *Toxicology*. 1997;117(2–3): 89–97.
50. Kappus H. Oxidative stress in chemical toxicity. *Arch Toxicol*. 19860(1–3):144–149.
51. Kjaer A, Laursen K, Thormann L, Borggaard O, Lebech PE. Copper release from copper intrauterine devices removed after up to 8 years of use. *Contraception*. 1993;47(4):349–358.
52. Cai S, Xia X, Zhu C, Xie C. Cupric ion release controlled by copper/low-density polyethylene nanocomposite in simulated uterine solution. *J Biomed Mater Res B Appl Biomater*. 2007;80(1):220–225.
53. Yu J, Li J, Li HG, Li JX, Xie CS, Zhu CH. Comparative study on contraceptive efficacy and clinical performance of the copper/low-density polyethylene nanocomposite IUD and the copper T220C IUD. *Contraception*. 2008;78(4):319–323.
54. Patai K, Dévényi L, Zelkó R. Comparison of surface morphology and composition of intrauterine devices in relation to patient complaints. *Contraception*. 2004;70(2):149–152.
55. Patai K, Berényi M, Sipos M, Noszál B. Characterization of calcified deposits on contraceptive intrauterine devices. *Contraception*. 1998;58(5):305–308.
56. Beltran-Garcia MJ, Espinosa A, Herrera I, Perez-Zapata AJ, Beltran-Garcia C, Ogura T. Formation of copper oxychloride and reactive oxygen species as causes of uterine injury during copper corrosion of Cu-IUD. *Contraception*. 2000;61(2):99–102.